

PRODUCTION OF K_2^0 MESONS AND NEUTRONS BY 10 GeV
AND 16 GeV ELECTRONS ON BERYLLIUM*

A. D. Brody, W. B. Johnson, D. W. G. S. Leith, G. Loew,
J. S. Loos, G. Luste, R. Miller, K. Moriyasu,
B. C. Shen, W. M. Smart and R. Yamartino

Stanford Linear Accelerator Center
Stanford University, Stanford, California

ABSTRACT

We have measured the K_2^0 yields at SLAC for electron energies of 10 and 16 GeV and at production angles of 2° and 4° , using the SLAC 40-inch hydrogen bubble chamber as a K_2^0 detector. The observed yields are compared with the predictions of a model involving the intermediate photo-production of $\phi(1020)$ mesons. In addition, we have measured the relative neutron to K_2^0 ratio as a function of the secondary beam momentum.

(Submitted to Phys. Rev. Letters)

* Work supported by the U. S. Atomic Energy Commission.

The yields of strongly interacting charged particles produced in electron-Be collisions have been measured recently at the Stanford Linear Accelerator Center by several groups¹⁻⁴ and confirm the general features of the calculations made by Tsai⁵ and others. We report here a measurement of the K_2^0 yields from Be for electron energies of 10 GeV and 16 GeV and production angles of 2° and 4° . The SLAC 40-inch hydrogen bubble chamber was used as the K_2^0 decay detector. The observed K_2^0 yields are consistent with the average of K^+ and K^- yields reported previously.^{1,2,4} A comparison with the K_2^0 yields expected from the photoproduction of $\phi(1020)$ mesons indicates that this process alone cannot explain either the observed magnitude or the angular dependence of the data. A preliminary measurement of the intensity and momentum spectrum of neutrons at the chamber indicates that favorable K_2^0 to neutron ratios may be obtained for secondary beam momenta above 2 GeV/c.

The primary electron beam from the accelerator was focused on a Be target which was mounted downstream of a vertical bending magnet. This magnet allowed variation of the production angle of the neutral beam within the range 1.5° to 5° . The intensity of the electron beam was measured by use of a toroid charge integrator. The position and focus of the electron beam at the target were continuously monitored by a closed circuit television display of a ruled zinc sulfide sheet attached to the upstream end of the Be target. The neutral beam passed through a sweeping magnet to clear out charged particles, a γ -ray filter,⁶ and the defining collimator. This collimator was a 1.2 meter Pb block placed 10 meters downstream from the Be target and had an angular acceptance of $12.5 \mu\text{sr}$. Additional sweeping magnets and shadowing collimators (non-defining) were located along the beam path to the bubble chamber which was situated 56 meters downstream of the target.

The intensity and momentum spectrum of the K_2^0 mesons at the chamber are simply related to the momentum distributions of the charged particles from the three-body K_2^0 decays in flight. In a method similar to that used by Firestone⁷ and Hopkins, Bacon, and Eisler⁸ we measured the momenta of the positive particle (\vec{P}_+) and the negative particle (\vec{P}_-) and tabulated the quantity P_{vis} , defined as $|\vec{P}_+| + |\vec{P}_-|$. Using Monte Carlo methods we then generated the expected P_{vis} distributions for each decay mode, corresponding to small intervals of incident K_2^0 momentum. Since the decay mode of individual events was not determined, the expected P_{vis} distributions were summed over the three charged decay modes (K_{e3} , $K_{\mu3}$, and $K_{\pi3}$) in proportion to their established rates.⁹ Finally, the incident K_2^0 momentum spectrum was iterated until the observed P_{vis} distribution could be reproduced satisfactorily. The resulting K_2^0 momentum spectra, within the statistical accuracy of this experiment, were completely insensitive to the parameters of the K_2^0 decays.¹⁰

Identification of K_2^0 decays and measurement of the quantity P_{vis} were done at the scan table. A physicist examined every recorded decay for acceptability; care was taken to eliminate electron pairs and decays associated with interactions in the chamber or in the entrance window. Subsequent precision measurement and spatial reconstruction of 100 accepted events indicated that the final sample contained ~6% non- K_2^0 decays. The measurement of P_{vis} was done using a circle template at the scan table since the method does not require high precision on individual measurements. A comparison to the 100 reconstructed events showed that individual template values of P_{vis} were accurate to within $\pm 10\%$.

Momentum spectra at the chamber were determined for 2° and 4° production angles, for 10 GeV and 16 GeV electrons incident on a 1.75 radiation length Be target. Two multiplicative factors were then applied to extrapolate the K_2^0 yields to the target; the first was the reciprocal of the probability that the K_2^0 will reach

the chamber before decaying,⁹ and the second was the attenuation factor of the beam in the thick γ -ray filter.⁶ The attenuation factor for lead was measured by placing an additional 130 gm/cm² of lead in the beam and repeating the measurement of the P_{vis} spectrum at 2^o for 16 GeV electrons. The shapes of the P_{vis} distributions for the two measurements were the same within statistical uncertainties; the absolute flux was reduced by a factor of 2.4 with the additional lead. The attenuation for tungsten was extrapolated from lead, and that for lithium hydride was estimated from K-nucleon cross sections¹¹ and from K^{\pm} -Be cross sections at 3.5 GeV/c.¹² The overall attenuation factor was 16 ± 5 .¹³

In Table I and in Fig. 1, we present the measured K_2^0 yields, corrected for K_2^0 decay and for beam attenuation. The uncertainties given include both statistical fluctuations and estimates for possible differences in relative normalization between the four spectra. The systematic uncertainty in attenuation ($\pm 35\%$) applies to all four spectra together and is not included in the table.

For comparison, the average of K^+ and K^- yields are also shown in Fig. 1. The 0^o data of Barna et al.,¹ (for 16 GeV electrons on a 1.8 r. l. Be target) agree very well with our yields. The data of Boyarski et al.,² at 1^o and 3^o (for 18 GeV electrons on an 0.3 r. l. Be target) have been extrapolated to a 1.75 r. l. Be target,¹⁴ and are consistent with our yields.

Yield estimates made by Tsai⁵ indicate that the most important single process for K_2^0 production is photoproduction of $\phi(1020)$ mesons which subsequently decay via $K_1^0 K_2^0$. However, many other processes may contribute, such as: $K^*(890)$ photoproduction, two-body or quasi-two-body processes (e. g. , $\gamma N \rightarrow K^0 Y$), or production by interactions of secondary pions within the target. To determine the relative importance of $\phi(1020)$ photoproduction, we have calculated expected K_2^0 yields¹⁵ for this process for our electron energies and production angles. The results of the

calculations are shown in Fig. 1 as dashed lines for 16 GeV electrons and as dotted lines for 10 GeV electrons. The magnitudes of the ϕ model curves are lower than our data, but more important, the drastic angular dependence predicted by the model is in contradiction to our experimental observations. Thus, we conclude that other processes are very important in K_2^0 production.

A preliminary measurement of the relative flux of neutrons to K_2^0 mesons at the chamber has been made. The ratio of the total number of K_2^0 mesons to the total number of neutrons incident at the chamber has been determined by a total interaction count. Denoting the neutron to K_2^0 ratio by R, one has:

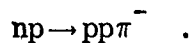
$$R = \left[(N_{\text{tot}} - N_K) / \sigma_n \right] / (N_K / \sigma_K)$$

where N_{tot} is the total number of interactions, N_K the number of expected K_2^0 induced interactions, and σ_K and σ_n are the $K_2^0 p$ and np total cross sections,¹⁶ respectively. The following values for R were found:

at 10 GeV	8.5 ± 1.7	at 2° ,
and	9.9 ± 2.0	at 4° ,
at 16 GeV	3.5 ± 0.6	at 2° ,
	4.0 ± 0.6	at 4° .

However, due to the strong momentum dependence of the neutron momentum distribution (shown below), only $\sim 10\%$ of the neutrons have momenta greater than 2 GeV/c.

A preliminary neutron momentum spectrum was measured from an analysis of three pronged interactions in the chamber. In this case, the neutral beam was produced at 2° by 16 GeV electrons incident on an 0.9 r.l. Be target. From this sample, 403 events were found which fitted the 3-constraint hypothesis:



The momentum distribution of neutrons at the chamber, presented in Fig. 2, was obtained by dividing the number of events observed in each momentum interval by

the cross section, $\sigma(np \rightarrow pp\pi^-)$.¹⁷ Also shown in Fig. 2 is the corresponding K_2^0 spectrum at the chamber.¹⁸ The relative normalization of the K_2^0 and neutron distributions is accurate to within 40%.¹⁹ As seen in the figure, the neutron momentum spectrum at the chamber peaks below 1.0 GeV/c and the neutron to K_2^0 ratio decreases by an order of magnitude over the neutral beam momentum range from 2 to 5 GeV/c.

ACKNOWLEDGEMENTS

We wish to thank A. Kilert, W. Walsh, R. Friday, D. McShurley, and A. Baumgarten for help in design and construction of the neutral beam, R. Watt and the bubble chamber staff, and our scanning and measuring staff. We are grateful for several discussions with Y. S. Tsai.

REFERENCES AND FOOTNOTES

1. A. Barna et al. , Phys. Rev. Letters 18, 360 (1967).
2. A. M. Boyarski et al. , SLAC Users Handbook, Stanford University, Stanford, California, revised version (1968) (unpublished).
3. A. Boyarski et al. , Phys. Rev. Letters 18, 363 (1967).
4. Stanley M. Flatté et al. , Phys. Rev. Letters 18, 366 (1967).
5. Y. S. Tsai, SLAC Users Handbook, Stanford University, Stanford, California (1966) (unpublished). References to previous work are given in this paper.
6. The γ filter consisted of 147 gm/cm^2 of tungsten, 173 gm/cm^2 of lead, and 50 gm/cm^2 of lithium hydride.
7. A. Firestone, thesis, Yale University (1967) (unpublished).
8. H. W. K. Hopkins, T. C. Bacon, and F. R. Eisler, Phys. Rev. Letters 19, 185 (1967).
9. All K_2^0 parameters used were taken from the compilation of the Particle Data Group, UCRL 8030, revised version (1968) (to be published in Rev. Mod. Phys.).
10. The analysis was done using the values 0, 0.022, and -0.25 for ξ, λ (parameters of the leptonic decays), and A (parameter for the $\pi^+ \pi^- \pi^0$ decay), respectively. Then the analysis was repeated using simple phase space for all decay modes. The K_2^0 spectra resulting from the two analyses agreed well within statistical uncertainties.
11. V. Cook et al. , Phys. Rev. Letters 7, 182 (1961); V. Cook et al. , Phys. Rev. 123, 320 (1961); A. N. Diddens et al. , Phys. Rev. Letters 10, 262 (1963); W. Galbraith et al. , Phys. Rev. 138, B913 (1965).
12. W. V. Hassenzahl, thesis, University of Illinois (1967) (unpublished).
13. This $\pm 35\%$ systematic uncertainty in attenuation completely dominates the systematic uncertainties due to solid angle or charge integration.
14. These extrapolations have been made from curves given in Ref. 5 and have normalization uncertainties of 20% to 40%.

15. Our calculation is identical to that made by U. S. Tsai et al., Phys. Rev. Letters 19, 915 (1967), with the exceptions that (1) the $\phi(1020)$ decays into $K_1^0 K_2^0$ rather than into $K^+ K^-$, and (2) the slope in t of the incoherent differential cross section is taken to be $5 (\text{GeV}/c)^{-2}$ rather than $10 (\text{GeV}/c)^{-2}$, as indicated by the recent $\phi(1020)$ photoproduction data of W. G. Jones et al., Phys. Rev. Letters 21, 586 (1968).
16. Values for $\sigma(K_2^0 p)$ and $\sigma(np)$ were taken to be 20 mb and 38 mb, respectively.
17. Measured values of $\sigma(np \rightarrow pp\pi^-)$ do not appear in the literature. Below 2.5 GeV/c, we have used the relation $\sigma(np \rightarrow pp\pi^-) = 1/2 \sigma(pp \rightarrow pp\pi^0)$ expected from the one pion exchange model with $I = 3/2$ dominance at the pion-nucleon scattering vertex. Above 2.5 GeV/c, we have used the relation $\sigma(np \rightarrow pp\pi^-) = \sigma(\bar{p}p \rightarrow \bar{n}p\pi^-)$ expected from the one pion exchange model. Values for $\sigma(pp \rightarrow pp\pi^0)$ were taken from: A. F. Dunaitsev and Y. D. Prokoshkin, Soviet Phys. JETP 36, 1179 (1959); D. V. Bugg et al., Phys. Rev. 133, B1017 (1964); K. R. Chapman et al., Phys. Letters 11, 253 (1964); F. F. Chen et al., Phys. Rev. 103, 211 (1956). Values for $\sigma(\bar{p}p \rightarrow \bar{n}p\pi^-)$ were taken from: T. Ferbel et al., Phys. Rev. 137, B1250 (1965); H. C. Dehne et al., Phys. Rev. 136, B843 (1964); K. Böckmann et al., Nuovo Cimento 42, 942 (1966); T. Ferbel et al., Phys. Rev. 173, 1307 (1968).
18. The K_2^0 spectrum at 2^0 for 16 GeV electrons has been extrapolated from 1.75 r.l. Be to 0.9 r.l. Be, using the curves given in Ref. 5.
19. The normalization of the neutron spectrum was determined by measuring R to be 3.2 ± 0.8 for the 0.9 r.l. data.

TABLE I
K₂⁰ YIELDS

Electron Energy, GeV	10		16	
Production Angle	2°	4°	2°	4°
No. Events in P _{vis} Distribution	930	717	877	931
K ₂ ⁰ Momentum Interval, GeV/c	Yield ^a at Target K ₂ ⁰ /e ⁻ /sr/GeV/c × 10 ⁻⁴			
1.0 - 1.5	0.74 ± 0.12	0.85 ± 0.15	1.35 ± 0.24	1.35 ± 0.23
1.5 - 2.0	0.96 ± 0.14	0.97 ± 0.13	1.75 ± 0.24	1.67 ± 0.22
2.0 - 2.5	1.10 ± 0.12	0.96 ± 0.13	2.02 ± 0.24	1.80 ± 0.21
2.5 - 3.0	1.10 ± 0.12	0.85 ± 0.11	2.17 ± 0.24	1.78 ± 0.19
3.0 - 3.5	0.99 ± 0.11	0.65 ± 0.09	2.18 ± 0.23	1.68 ± 0.18
3.5 - 4.0	0.82 ± 0.09	0.46 ± 0.07	2.14 ± 0.23	1.54 ± 0.17
4.0 - 4.5	0.60 ± 0.08	0.29 ± 0.05	2.00 ± 0.22	1.35 ± 0.15
4.5 - 5.0	0.40 ± 0.05	0.17 ± 0.04	1.78 ± 0.21	1.13 ± 0.12
5.0 - 5.5	0.24 ± 0.04	0.09 ± 0.03	1.55 ± 0.19	0.93 ± 0.10
5.5 - 6.0	0.13 ± 0.03		1.31 ± 0.16	0.74 ± 0.08
6.0 - 6.5	0.07 ± 0.03		1.10 ± 0.13	0.58 ± 0.07
6.5 - 7.0			0.89 ± 0.12	0.45 ± 0.06
7.0 - 7.5			0.72 ± 0.09	0.34 ± 0.06
7.5 - 8.0			0.56 ± 0.08	0.26 ± 0.06
8.0 - 8.5			0.44 ± 0.07	0.19 ± 0.05
8.5 - 9.0			0.33 ± 0.06	0.14 ± 0.04
9.0 - 9.5			0.26 ± 0.06	
9.5 - 10.0			0.19 ± 0.05	
10.0 - 10.5			0.15 ± 0.04	

a. Errors quoted in this table do not include the overall uncertainty of ± 35% (see text).

FIGURE CAPTIONS

1. Yields of K_2^0 mesons from a 1.75 r.l. Be target measured for the following electron energies and production angles: (○) 16 GeV, 2^0 ; (●) 16 GeV, 4^0 ; (△) 10 GeV, 2^0 ; and (▲) 10 GeV, 4^0 . Shown for comparison are the average of K^+ and K^- yields previously measured under the following conditions: (X) 0^0 production with 16 GeV electrons on a 1.8 r.l. Be target (Ref. 1); (□) 1^0 production and (■) 3^0 production with 18 GeV electrons on an 0.3 r.l. Be target (Ref. 2). The measurements of Ref. 2 have been extrapolated from 0.3 r.l. to 1.75 r.l. Be target. Predicted contributions from $\phi(1020)$ photo-production are shown for electron energies and production angles of: 16 GeV, 2^0 (upper dashed curve); 16 GeV, 4^0 (lower dashed curve); 10 GeV, 2^0 (upper dotted curve); and 10 GeV, 4^0 (lower dotted curve).
2. Comparison of the neutron and K_2^0 fluxes at the HBC for 2^0 production with 16 GeV electrons.

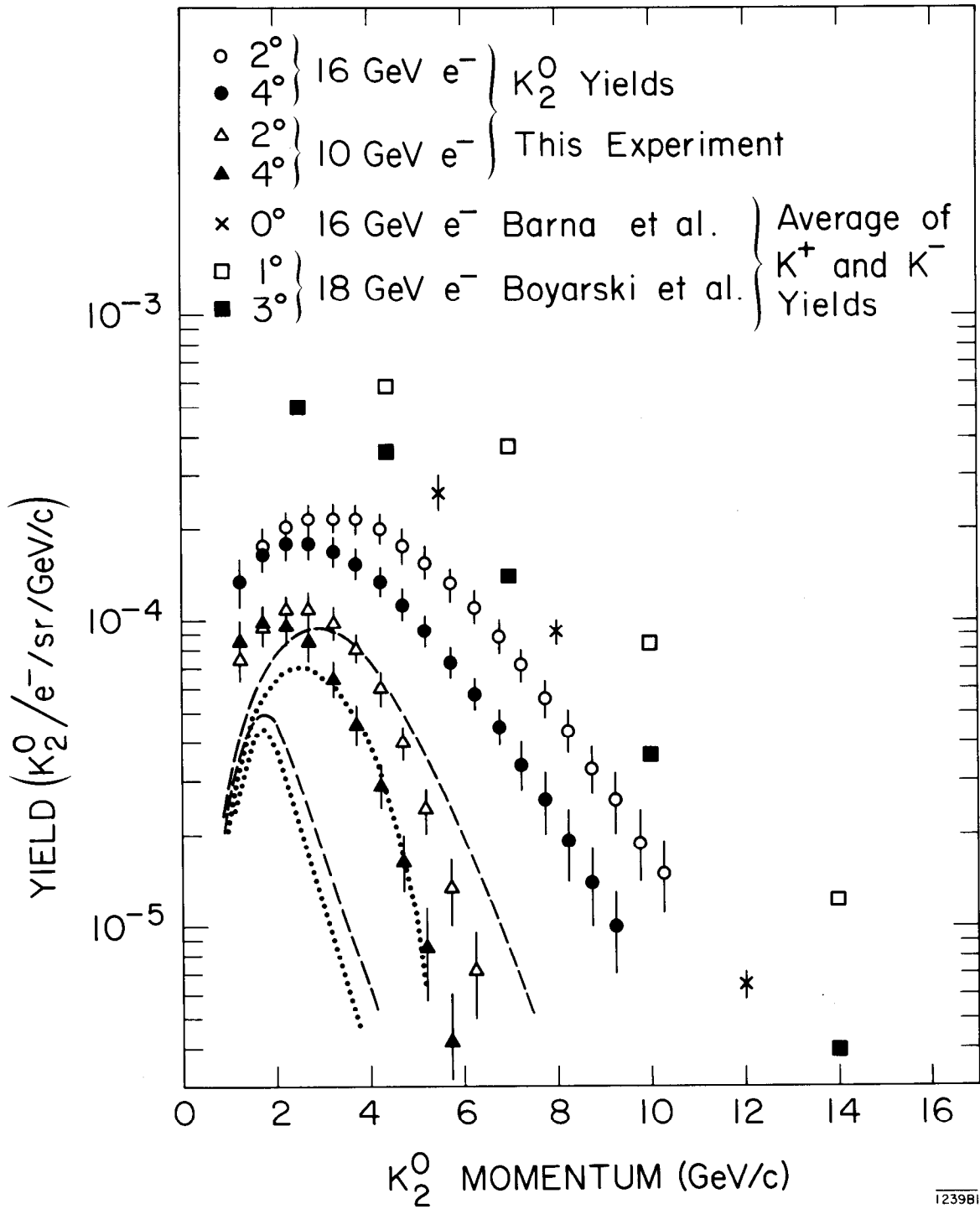


Fig. 1

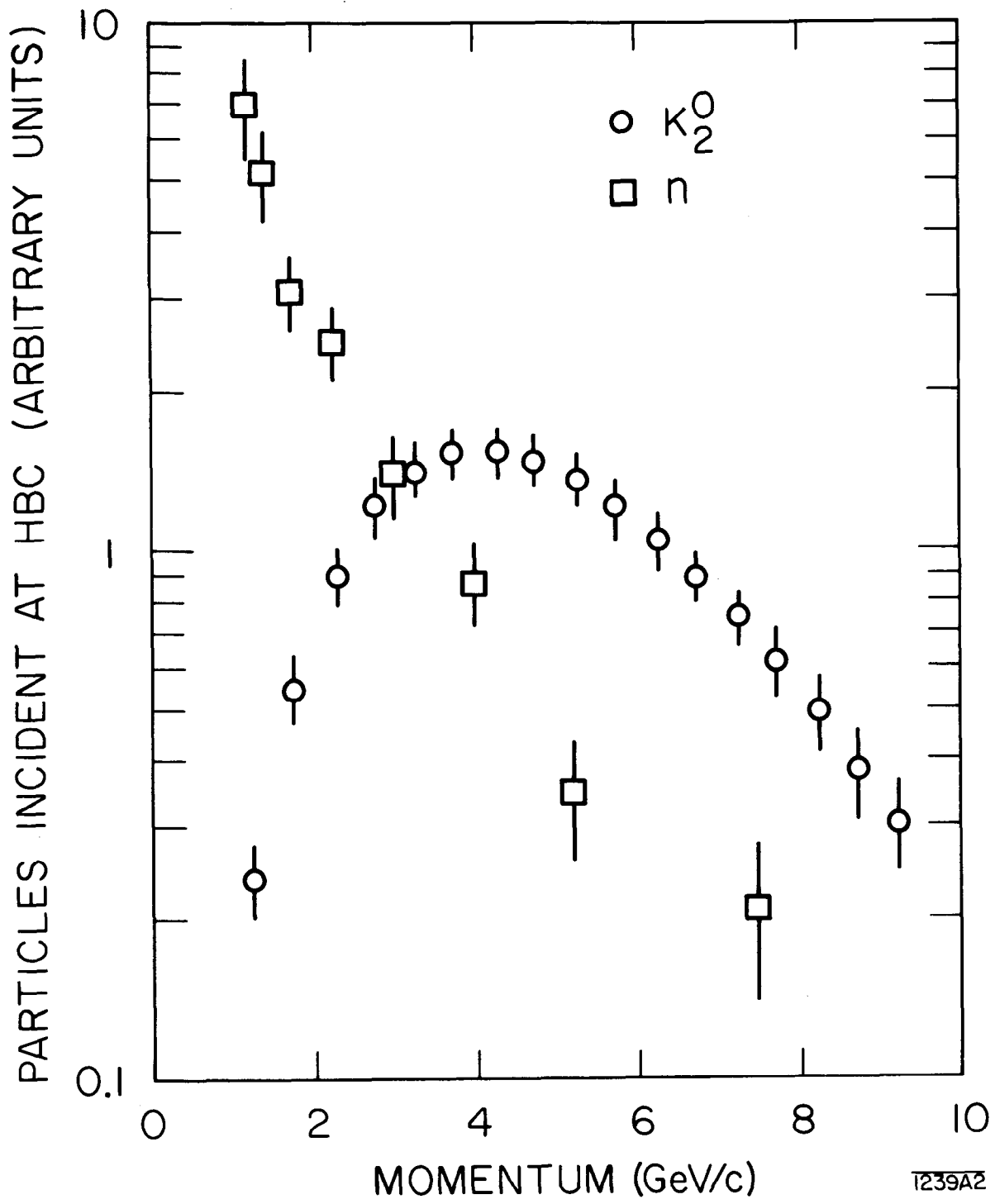


Fig. 2